SLAC-PUB-6514
May 1994
T/E

NOTES ON THE LANDAU, POMERANCHUK, MIDGEL EFFECT: EXPERIMENT AND THEORY*

Martin L. Perl
Stanford Linear Accelerator Center,
Stanford University,
Stanford, California 94309

Abstract

The status of the Landau, Pomeranchuk, Migdal Effect is briefly reviewed. A recent experiment at the Stanford Linear Accelerator Center substantially agrees with the existing theoretical formulation. However, that formulation suffers from an imprecise foundation and a lack of generality. The difficulty of finding a simple, explanatory picture of the $1/\sqrt{k}$ behavior of the Effect is also noted.

Talk presented at:
LES RENCONTRES DE PHYSIQUE DE LA VALLEE D'AOSTE,
La Thuile, Italy – March 6–12, 1994

*This work was supported by the Department of Energy, contract DE–AC03–76SF00515.

I. Introduction and Bethe-Heitler Bremsstrahlung Theory

In 1993 a group of colleagues and myself[1,2,3,4] carried out the first precise experiment on the Landau, Pomeranchuk, Migdal Effect (LPM Effect).[5,6,7,8] This effect occurs when an ultrarelativistic particle emits low energy bremsstrahlung photons as the particle passes through dense matter; fewer photons are emitted than predicted by bremsstrahlung theory for isolated atoms. Our measurements are in substantial agreement with existing LPM Effect theory as developed by Migdal[6]

However, our use of this theory has accentuated the limitations of this theory. In Sec. II I give a qualitative description of the theory, its predictions, and its limitations. I also note the problem of finding a simple, semi-quantitative picture of the effect; a picture which could be useful in thinking about the underlying physics. In the final section, Sec. III, I summarize our first analyzed experimental results.[2,4]

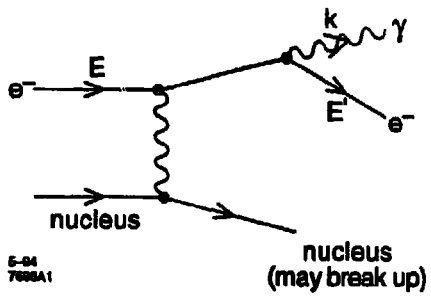

Fig. 1. Bremsstrahlung process on an isolated atom.

I begin by considering the cross section for bremsstrahlung by an ultrarelativistic electron of mass m and energy E on an isolated atom with nuclear charge Z (Fig. 1). The criteria for ultrarelativistic in this case is not only $E/m = \gamma \gg 1$, but also the criteria given in Eq. B4 of Tsai.[9] Next, let k be the photon energy and use the complete screening approximation[9] so that

$$k \ll E \tag{1}$$

is required.

Then, the differential cross section is[9)]

$$\frac{d\sigma}{dk} = 4\alpha r_e^2 \frac{1}{k} \times \left\{ \left[\frac{4}{3} - \frac{4}{3}y + y^2 \right] \left[Z^2 F_{el} + Z F_{inel} \right] + \frac{1}{9} [1-y][Z^2+Z] \right\} \tag{2}$$

Here $y = k/E$, α is the fine structure constant, and r_e is the classical radius of the electron. In terms of the electron charge e and mass m.

$$r_e = \frac{e^2}{mc^2} = 2.82 \times 10^{-13} \text{ cm} \tag{3}$$

In Eq. (2) there has already been integration over the other kinematic variables of the photon, scattered electron, and produced hadrons. F_{el} and F_{inel} are the results of this integration over the elastic and inelastic atomic from factors[9)], they do not depend on y or E, and are given approximately by[9)]

$$F_{el} = \ell n \left(\frac{184}{Z^{1/3}} \right) \ , \ F_{inel} = \ell n \left(\frac{1194}{Z^{2/3}} \right) \tag{4}$$

Therefore when $y \ll 1$, Eq. (2) becomes the well known.

$$\left(\frac{d\sigma}{dk} \right)_{y \ll 1} \approx \frac{\text{constant}}{k} \tag{5}$$

I define for later use the probability per unit length of emitting a photon with energy between k and $k + dk$

$$P_{BH} = n \frac{d\sigma}{dk} = 4n\alpha r_e^2 \frac{1}{k} \times \left\{ \left[\frac{4}{3} - \frac{4}{3}y + y^2 \right] \left[Z^2 \ell n \left(\frac{184}{Z^{1/3}} \right) + Z \ell n \left(\frac{1194}{Z^{2/3}} \right) \right] + \frac{1}{9} [1-y] [Z^2+Z] \right\} \tag{6a}$$

The subscript BH denotes the Bethe-Heitler bremsstrahlung theory and n is the number of atoms per unit volume. For future use I note that if we ignore the $Z \ell n \left(\frac{1194}{Z^{2/3}} \right)$ term and the $Z^2 + Z$ terms in Eq. (6a) and set $y \ll 1$

$$P_{BH} = 4n\alpha r_e^2 Z^2 \ell n \left(\frac{184}{Z^{1/3}} \right) \frac{1}{k}$$

Using the radiation length X_0 defined approximately by

$$X_0^{-1} \approx 4n\alpha r_e^2 Z^2 \ell n \left(\frac{184}{Z^{1/3}} \right) \tag{6b}$$

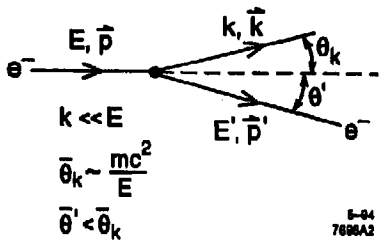

Fig. 2. Kinematic quantities for $k << E$.

$$P_{BH} = \frac{1}{X_0 k} \tag{6c}$$

Also I note, although I have not discussed the angular distributions, that the average values of the angle θ_k and θ' (Fig. 2) are

$$\begin{aligned} \bar{\theta}_k &\sim \frac{mc^2}{E} \\ \bar{\theta}' &\lesssim \bar{\theta}_k \end{aligned} \tag{7a}$$

when

$$y \ll 1 \tag{7b}$$

that is, when $k \ll E$. The longitudinal momentum transfer, Fig. 2, is

$$q_{\|} = p - p' \cos\theta' - \frac{k}{c} \cos\theta_k \ ,$$

and for the conditions in Eqs. (7) simplifies to

$$q_{\|} \approx p - p' - k/c \approx \frac{(mc^2)^2 k}{2EE'c} \approx \frac{k}{2\gamma^2 c} \tag{8}$$

where $\gamma = E/mc^2$. The c appears in Eq. (8) because k is an energy.

The uncertainty principle requires that the spatial position of the bremsstrahlung process have a longitudinal spatial uncertainty of

$$\ell_{\|} \approx \frac{\hbar}{q_{\|}} \approx \frac{2\hbar c\gamma^2}{k} \tag{9}$$

If the atom taking part in the process is isolated from all other atoms by distances greater than $\ell_\parallel$, the uncertainty principle has no effect. However, if the atom is not isolated then Eq. (9) can not be ignored, and it leads to the LPM Effect.

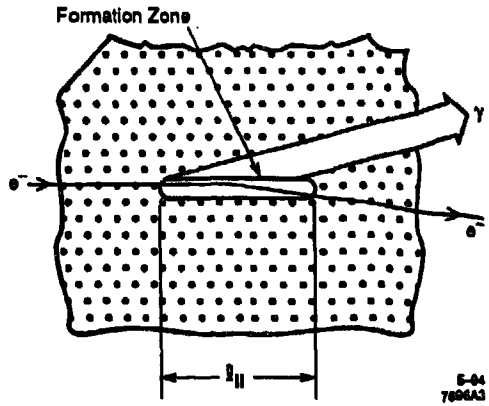

Fig. 3. A qualitative picture of the LPM Effect.The bremsstrahlung γ is produced coherently over the entire length $\ell_\parallel$ of the formation zone. The multiple scattering of the e^- inside the formation zone suppresses the bremsstrahlung probability.

II. The Migdal Formulation of the LPM Effect

Suppose the brehmsstrahlung process just described occurs in a dense medium, Fig. 3, such that

$$\ell_\parallel \gg 1/\sqrt[3]{n} \tag{10}$$

Then the point of occurrence of the brehmsstrahlung process is uncertain within the formation zone shown in Fig. 3.

Any process which changes the path of the electron inside the distance $\ell_\parallel$ will reduce P, the probability per unit length of bremsstrahlung emission. Of course, the process most likely to occur is multiple scattering by the incident or final electron on the atoms in the formation zone.

Consider the simple equation for the mean square multiple scattering angle over a length ℓ,

$$\overline{\theta_s^2} = \left(\frac{E_s}{E}\right)^2 \frac{\ell}{X_0} \tag{11}$$

where X_0 is a radiation length and $E_s = \sqrt{\frac{4\pi}{\alpha}}mc^2 = 21$ MeV. The bremsstrahlung probability

per unit length, P, will be reduced when

$$\overline{\theta_s^2} \gtrsim \bar{\theta}_k^2 = \left(\frac{mc^2}{E}\right)^2 \tag{12}$$

Using $\overline{\theta_s^2} = \bar{\theta}_k^2$ define

$$\ell_{LPM} = \left(\frac{mc^2}{E_s}\right)^2 X_0 \tag{13}$$

Then Eq. 12 leads to the condition

$$\ell_{\parallel} \gtrsim \ell_{LPM} \tag{14}$$

for reduction of P by multiple scattering. Table 1 gives some examples of ℓ_{LPM} and $\ell_{\parallel}$ for our experiment.[2)]

Table 1. Values of X_0 and ℓ_{LPM}. Values of k_{LPM} for 25 GeV incident electrons.

Material	Z	X_0	ℓ_{LPM} (μm)	k_{LPM} (MeV)
C	6	18.8	109	8.6
Fe	26	1.76	10.2	92
Au	79	0.33	1.9	490
U	92	0.32	1.9	510

A first problem in working with the LPM effect is to try to develop a physical picture as to how and why the reduction of P occurs under conditions of Eq. (12). Qualitatively the bremsstrahlung photon has to be emitted by a coherent process over the length $\ell_{\parallel}$. The repeated changing of electron direction due to multiple scattering inside $\ell_{\parallel}$ destructively interferes with that coherence. Galitsky and Gurevich[10)] have presented a quantitative picture of the LPM effect which I recommend to the reader.

Indeed other processes which destructively interfere with that coherence also reduce P. One example is the effect of a magnetic field changing the electron's direction. Another example is photon absorption, or scattering in the medium. However, this paper is restricted to the multiple scattering effect.

Migdal[6)] has provided a derivation of P_{LPM} which replaces P_{BH} (Eq. 6). But the derivation is much too complicated to summarize here and I know of no simpler quantitative derivation. Therefore, I proceed to his results. Using Eq. (14), the LPM Effect requires

$$\frac{\ell_{LPM}}{\ell_{\parallel}} \lesssim 1 \tag{15a}$$

where

$$\frac{\ell_{LPM}}{\ell_{\parallel}} = \frac{\alpha k X_0}{8\pi\hbar c\gamma^2} = y\left(\frac{mc}{\hbar}\right)\left(\frac{mc^2}{E}\right)\frac{\alpha X_0}{8\pi} \tag{15b}$$

From Eqs. (15), the LPM effect requires

$$k \lesssim \frac{8\pi\hbar c\gamma^2}{\alpha X_0} = k_{LPM} \tag{16a}$$

With X_0 in cm

$$k_{LPM} = 6.78 \times 10^{-8}\gamma^2/X_0 \text{ MeV} \tag{16b}$$

Table 1 gives values of k_{LPM} for $E = 25$ GeV. Remember that $k \lesssim k_{LPM}$ is not a sharp criterion. Within a factor of 2 or so, when k falls below k_{LPM} the LPM Effect begins to reduce the bremsstrahlung probability.

Migdal uses a dimensionless variable

$$s = \frac{1}{2}\left[\frac{y}{1-y}\right]^{\frac{1}{2}}\left[\frac{mc}{\hbar}\frac{mc^2}{E}\frac{\alpha X_0}{8\pi\xi(s)}\right]^{1/2} \tag{17a}$$

There are two differences between Eq. (17a) and $\sqrt{\ell_{LPM}/\ell_{\parallel}}$ from Eq. (15b). First, there is the function:

$$\begin{aligned} \xi(s) &= 1 \quad , \quad s > 1 \\ 1 < \xi(s) &< 2 \quad , \quad s < 1 \end{aligned} \tag{17b}$$

Second there is the $1 - y$ term in the first bracket, which is unimportant when $y \ll 1$. Thus, for $y \ll 1$, s is proportional to $\sqrt{\ell_{LPM}/\ell_{\parallel}}$ within a factor $\sqrt{2}$, hence

$$\begin{aligned} s \gg 1 &: \text{ no LPM Effect} \\ s \ll 1 &: \text{ strong LPM Effect} \end{aligned} \tag{17c}$$

Migdal replaces $\alpha X_0/\pi$ by

$$B = 2\pi Z^2 r_e^2\, n\, \ell n\left(\frac{183}{Z^{\frac{1}{3}}}\right)\xi(s) = \frac{\pi\xi(s)}{2\alpha X_0} \tag{18}$$

and writes

$$s = \frac{1}{8}\left[\frac{y}{1-y}\frac{m^2c^3}{\hbar E}\frac{1}{B}\right]^{\frac{1}{2}} \tag{19}$$

Having defined s and B and indicated their significance. I now give the Migdal replacement for P_{BH} in Eq. (6).

$$P_{LPM} = \frac{2\alpha B}{3\pi k} \left\{ y^2 G(s) + 2 \left[1 + (1-y)^2 \right] \phi(s) \right\} \tag{20}$$

where for

$$\begin{array}{lll} s \to 0 & \phi(s) \to 6s & G(s) \to 12\pi s^2 \\ s \to \infty & \phi(s) \to 1 & G(s) \to 1 \end{array} \tag{21}$$

Therefore where $s \to \infty$

$$P_{LPM} = 4n\alpha r_e^2 \frac{1}{k} \left[\frac{4}{3} - \frac{4}{3} y + y^2 \right] \left[Z^2 \ell n \frac{183}{Z^{\frac{1}{3}}} \right] \tag{22}$$

Comparing this with P_{BH}, Eq. (6a) we see almost the same formula except two small terms are missing:

$$Z\ell n \left(\frac{1194}{Z^{2/3}} \right) \ , \ \frac{1}{9} \left[1 - y \right] \left[Z^2 + Z \right] \tag{23}$$

When $s \ll 1$ and with the approximation $\xi(s) \approx 1$, Eq. (20) becomes

$$\begin{aligned} P_{LPM} &\approx \frac{8\alpha}{\pi k} Bs \left[1 + (1-y)^2 \right] \\ P_{LPM} &\approx \frac{\alpha}{\pi} \left[\frac{m^2 c^3}{\hbar} \frac{B}{kE(E-k)} \right]^{1/2} \left[1 + (1-y)^2 \right] \end{aligned} \tag{24}$$

Looking at Eq. (24) we see that for $s \ll 1$ and $y \ll 1$, P_{LPM} is proportional to $1\sqrt{k}$. This is in sharp contrast to P_{BH} which for $y \ll 1$ is proportional to $1/k$. To emphasize this point, I set $y \ll 1$ in Eq. (24), then

$$P_{LPM} \approx \frac{2\alpha}{\pi} \left[\frac{m^2 c^3}{\hbar E^2} \frac{B}{k} \right]^{1/2}$$

and using from Eq. (18), $B \approx \pi / 2\alpha X_0$

$$P_{LPM} \approx \sqrt{\frac{2\alpha}{\pi}} \frac{mc^2}{E} \left[\frac{1}{\hbar c X_0 k} \right]^{1/2} , \ s \ll 1, y \ll 1 \tag{25a}$$

Contrast this to a simplified form of Eq. (6a) with $y \ll 1$ and the term in Eq. (23) ignored, namely Eq. (6c)

$$P_{BH} \approx \frac{1}{X_0 k} \ , \ y \ll 1 \tag{25b}$$

Comparing Eqs. (25a) and (25b) we note in addition to the $1/\sqrt{k}$ change from $1/k$ other differences. P_{LPM} is proportional to $1/E$ whereas P_{BH} is independent of E in these approx-

imations. P_{LPM} is proportional to $\sqrt{n}$ whereas P_{BH} is proportional to n. Here n is the number of atoms per unit volume.

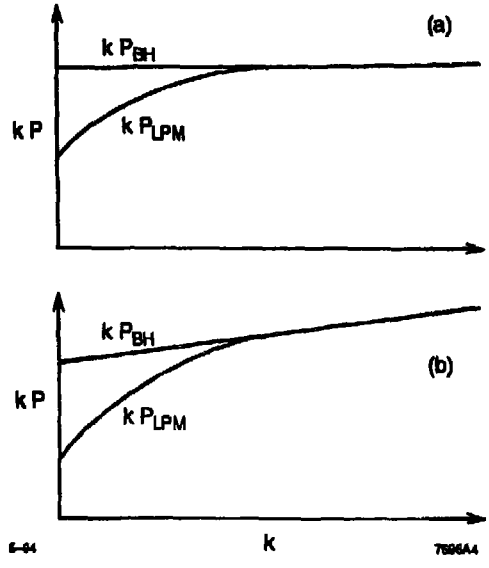

Fig. 4. A comparison of the theoretical curves for kP_{BH} and kP_{LPM} for (a) an ideal experiment, and (b) our experiment in which the e^- may emit more than 1 photon while passing through the target.

Remember that Eq. (25a) is for $s \ll 1$ and is the extreme form of the LPM Effect caused by multiple scattering. The more general form of P_{LPM} is Eq. (20), and for $s \gg 1$ $P_{LPM} \to P_{BH}$. This is pictured graphically in Fig. 4a where kP is plotted against k. The kP_{BH} curve is a horizontal straight line as long as $k \ll E$. The kP_{LPM} curve falls below kP_{LPM} when $k \gtrsim k_{LPM}$ as defined in Eqs. (16).

As I describe in the next section, our experiment[2,3,4] is in substantial agreement with the Migdal formulation of the LPM Effect. Nevertheless, there are a number of problems in this formulation. First, the derivation in Midgal's paper[6] has many approximations, I was not able to estimate their validity. Indeed I am surprised the formulas work so well. Second, Migdal's formulation at large s does not agree perfectly with Bethe-Heitler theory, his P_{LPM} does not have the terms listed in Eq. (23). Third, the Migdal formulation is for a medium of infinite extent along the electron trajectory, it does not possess any direct way of calculating the boundary effect described in the next section. Fourth, there is no physical insight for the

$1/\sqrt{k}$ behavior of P_{LPM} at $s \ll 1$. In terms of dimensions, the $1/\sqrt{k}$ is taken care of by

$$\left(\frac{1}{\hbar c X_0 k}\right)^{1/2} = \frac{1}{\hbar c}\left(\frac{\hbar c/X_0}{k}\right)^{1/2}$$

so that P_{LPM} in Eq. (25a) has the proper dimensions of (energy length)$^{-1}$. But why $k^{1/2}$?

Therefore, more work is needed to provide a more precise foundation, more physical insight, and a more general formulation for the LPM Effect. Meanwhile, as we will show in the next section, the Migdal formulation works quite well.

III. Experiment

The only direct measurement previous to ours[2,3,4] is that of Varfolomeev *et al.*[11] published in 1976. However, the results of Varfolomeev *et al.* are limited in the range of k and they are difficult to use for tests of the theory because they are given in terms of ratios of bremsstrahlung spectra for pairs of materials.

Our experiment[3] was carried out in 1993 in End Station A of the Stanford Linear Accelerator Center. We used 25 GeV to 400 MeV electron beams with an average intensity of one electron per pulse and 120 pulses per second. These beams were obtained parasitically from the Stanford Linear Collider (SLC) beams while the SLC was operating for the SLD e^+e^- annihilation experiment at the Z^0 energy.

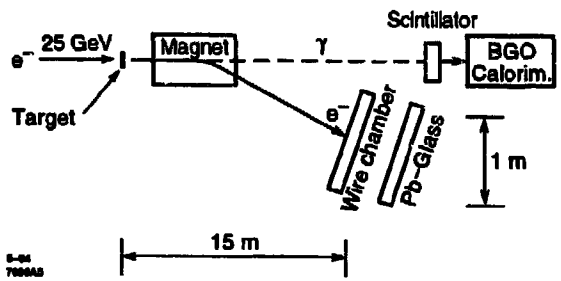

Fig. 5. Schematic picture of the experiment.

Figure 5 shows the experimental arrangement.[2] Targets of 1% to 6% of a radiation length of C, Al, Fe, W, Au, Pb, and U were used, 0.1% of a radiation length was also used for Au. The bremsstrahlung photon was detected in a downstream BGO calorimeter and the scattered e^- was bent in a 3.25 T-m magnet and detected in a wire chamber and a Pb-glass calorimeter. Hence, both k and E' were measured.

In this note I reproduce our results for E=25 GeV electrons on C, Au, and U targets for $5 < k < 500$ MeV. In order to compare our measurements with the Migdal formulation we must note that sometimes an e^- will emit more than 1 photon in passing through the target. For example, if two photons of energies k_1, and k_2 are emitted, the BGO calorimeter measures the sum $k_1 + k_2$ and the scattered e^- has energy $E' = E - (k_1 + k_2)$. This multiple photon emission depletes $d\sigma/dk$ for small k and enhances $d\sigma/dk$ at large k. Hence the ideal kP_{BH} and kP_{LPM} spectra in Fig. 4a are distorted in the data to the curves in Fig. 4b.

The comparison of our measurements for 25 GeV e^- and C, Au, and U targets with Bethe-Heitler theory (BH) and Landau, Pomeranchuk, Migdal theory (LPM) are given in Figs. 6, 7, 9, and 10. The cross section units, kdN/dk, are photons per bin (with 25 bins per decade) per 1000 photons with k in MeV. Normalization and errors are discussed in Ref. 2.

Figures 6, 7a, and 7b clearly show the LPM effect and demonstrate that LPM theory is in much better agreement with the data than BH theory. We see that the Migdal formulation of LPM theory is reasonably well verified. But as is most clear in Figs. 7a and 7b, there is not perfect agreement at the smaller values of k, in that region $(kdN/dk)_{measured} > (kdN/dk)_{LPM}$.

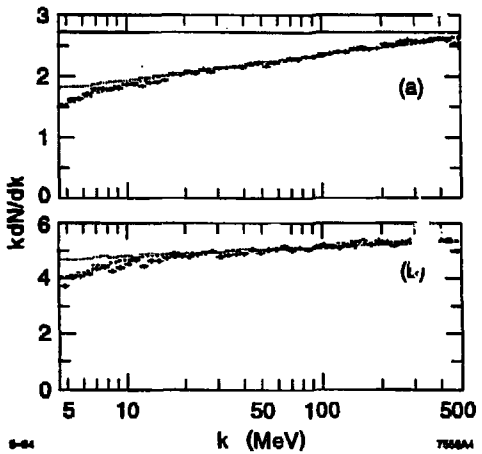

Fig. 6. kdN/dk in number photons per bin per 1000 electrons versus k in MeV for 25 GeV electrons incident on (a) 2% and (b) 6% radiation length carbon targets. Our measurements are denoted by crosses, the Bethe-Heitler theory prediction is denoted by the dotted histogram, upper curve, and the Landau, Pomeranchuk, Migdal theory prediction is denoted by the dashed histogram, lower curve. The latter is a better fit to the measurements.

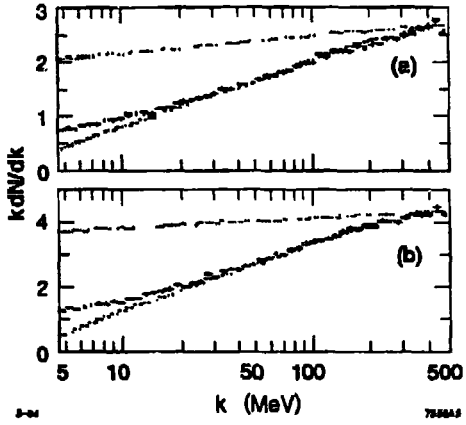

Fig. 7. kdN/dk in number photons per bin per 1000 electrons versus k in MeV for 25 GeV electrons incident on (a) 3% and (b) 5% radiation length uranium targets. Our measurements are denoted by crosses, the Bethe-Heitler theory prediction is denoted by the dotted histogram, upper curve, and the Landau, Pomeranchuk, Migdal theory prediction is denoted by the dashed histogram, lower curve. The latter is a better fit to the measurements.

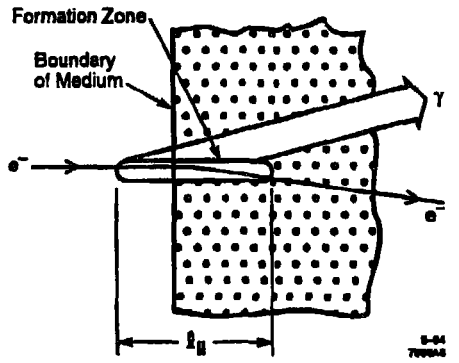

Fig. 8. A qualitative picture of the LPM Effect when the formation zone extends beyond the boundary of the radiating medium.

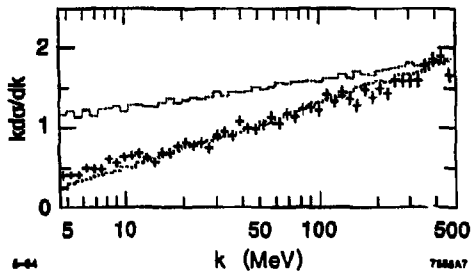

Fig. 9. kdN/dk for a 5% radiation length uranium target minus kdN/dk for a 3% radiation length uranium target. Our measurements are denoted by crosses, the Bethe-Heitler theory prediction is denoted by the dotted histogram, upper curve, and the Landau, Pomeranchuk, Migdal theory prediction is denoted by the dashed histogram, lower curve. The subtraction of the two spectra roughly removes the boundary effect and brings the Landau, Pomeranchuk, Migdal theory prediction closer to the measurements.

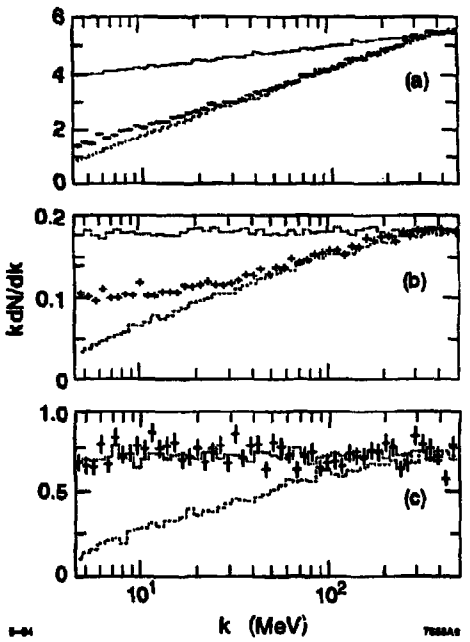

Fig. 10. kdN/dk in number photons per bin per 1000 electrons versus k in MeV for 25 GeV electrons incident on (a) 6%, (b) 1%, and (c) 0.1% radiation length uranium targets. Our measurements are denoted by crosses, the Bethe-Heitler theory prediction is denoted by the dotted histogram, upper curve, and the Landau, Pomeranchuk, Migdal theory prediction is denoted by the dashed histogram, lower curve. As the target becomes thinner the spectrum passes from the Landau, Pomeranchuk, Migdal Effect regime to the isolated atom regime.

We think that this disagreement may be caused by the failure of the Migdal formulation to account for the boundary of the target. As pictured in Fig. 8, when the formation zone of length $\ell_{\|}$ overlaps the boundary of the material, there will be less reduction of the bremsstrahlung probability. Fig. 9 demonstrates the plausibility of this boundary effect by showing for U.

$$\left(\frac{kdN}{dk}\right)_{5\%\,X_0\,target} - \left(\frac{kdN}{dk}\right)_{3\%\,X_0\,target}$$

The boundary effect is now subtracted out and there is better agreement between the data and the LPM theory prediction.

Figures 10 for Au with 6% X_0, 1% X_0 and 0.1% X_0 target is a dramatic demonstration of the transition from LPM theory conditions to BH theory conditions. As the target thickness decreases the boundary effect becomes more important. For a very thin target, the boundary effect cancels out the LPM suppression and we are back to the case of an isolated atom.

Thus our experiment has clearly demonstrated the existence of the LPM Effect and has in large part verified the Migdal formulation. We have two large remaining tasks, we have to complete the analysis of our data and we have to refine or improve the theory so that we can make more straightforward comparison of experiment and theory. An important part of improving the theory concerns yet smaller values of k where the LPM Effect must include dielectric suppression, the reduction of bremsstrahlung probability due to interaction of the photon with the medium.

IV. Acknowledgement

I wish to thank my colleagues on the experiment described in Sec. III and particularly to acknowledge Spencer Klein who conceived the experiment.

References

1. The experiment was carried out by S.R. Klein, M. Cavalli-Sforza, L.A. Kelly of the University of California at Santa Cruz; P. Anthony, R. Becker-Szendy, L.P. Keller, G. Niemi, L.S. Rochester, and M.L. Perl of the Stanford Linear Accelerator Center, Stanford University; and P.E. Bosted and J.White of the American University.
2. S.R. Klein *et al.*, *Proc. XVI Int. Symp. Lepton and Photon Interactions at High Energies* (Ithaca, 1993), Eds. P. Drell and D. Rubin, p. 172.
3. R. Becker-Szendy *et al.*, SLAC-PUB-6400 (1993), to be published in *Proc. 21st SLAC Summer Institute on Particle Physics.*
4. M. Cavalli-Sforza *et al.*, SLAC-PUB-6387 (1993), to be published in the *Trans. IEEE 1993 Nucl. Sci. Symp..*
5. L.D. Landau and I.J. Pomeranchuk, Dokl.Akad.Nauk. SSSR **92**, 535 (1953); **92**, 735 (1953). These two papers are available in English in L. Landau, *The Collected Papers of L.D. Landau*, Pergamon Press, 1965.
6. A.B. Migdal, *Phys. Rev.* **103**, 1811 (1956).
7. E.L. Feinberg and I. Pomeranchuk, *Nuovo Cimento*, Supplement to Vol. **3**, 652 (1956).
8. J.S. Bell, *Nuclear Physics* **8**, 613 (1958)
9. Y.-S. Tsai, *Rev. Mod. Phys* **46**, 815 (1974).
10. V.M. Galitsky and I.I. Gurevich, *Il Nuovo Cimento* **32**, 396 (1964).
11. A.A. Varfolomeev *et al.*, *Sov. Phys. JETP* **42**, 218 (1976).